Giant electron-spin g factors in a ferromagnetic nanoparticle

P. Gartland, F. T. Birk, W. Jiang, and D. Davidović

Phys. Rev. B **88**, 075303 — Published 5 August 2013

DOI: 10.1103/PhysRevB.88.075303

Giant Electron-Spin-g-factors in a Ferromagnetic Nanoparticle

P. Gartland,* F.T. Birk, W. Jiang, and D. Davidović
School of Physics, Georgia Institute of Technology, Atlanta, GA 30332
(Dated: July 18, 2013)

We utilize single-electron tunneling spectroscopy to measure the discrete energy levels in a nanometer-scale cobalt particle at T=60mK, and find effective single-electron spin g-factors ≈ 7.3. These large g-factors do not result from the typical orbital contribution to g-factors, since the orbital angular momentum is quenched. Instead, they are due to non-trivial many-body excitations. A kink in the plot of conductance vs. voltage and magnetic field is a signature of degenerate total spin on the particle. Spin-Orbit interactions cause the new particle eigenstates to have 'spin' that is an admixture of pure spin states. Fluctuations in the discrete energy level spacing allow for the total change in 'spin' on the particle during a single-electron tunneling event to be $\Delta S' = 3/2$, leading to a g-factor around 6.

PACS numbers: 73.23.Hk,73.63.Kv,73.50.-h

INTRODUCTION

The g-factor of an elementary particle is a dimensionless parameter relating the magnetic moment and the angular momentum. For an electron, the magnetic moment due to spin $\vec{S}$ is $\vec{\mu} = -g\mu_B\vec{S}/\hbar$, where g is the spin g-factor, μ_B is the Bohr Magneton, and $\hbar$ is the reduced Planck constant. In the Dirac point particle model of an electron, the spin g-factor is precisely 2, but the coupling to the environment can change that value. Recently, g-factors were measured of single electrons occupying quantum electron-in-a-box levels in a nanometer-scale metallic particle . [1–9] In particles made from light metals such as Al, the g-factors are very close to 2, demonstrating that the g-factors are (very nearly) spin g-factors, and that coupling between the spin and the environment is weak. The orbital motion of the electron does not affect the g-factors in light metallic particles because of the quenching of the orbital angular momentum. [10, 11] Introduction of heavier metals into the particle material leads to a significant reduction of the g-factor, caused by the coupling between the electron spin and the crystalline environment, via the Spin-Orbit (SO) interaction. [1, 2]

Here we present measurements of electron g-factors $g \approx 7.3$ in a ferromagnetic (Cobalt) particle. We show how this strong enhancement arises from the coupling between traditional electron-in-a-box levels and the many-body states in the electronic environment, when the ground state of the particle is nearly spin-degenerate. A different mechanism leading to very large spin g-factors has been proposed for normal metal particles, but large g-factors have not been confirmed until now, probably because of the weak electron-electron interactions in normal metals. [12, 13] By switching the material from normal metal to a ferromagnet, the electron-electron interactions strengthen, making it more probable to observe large g-factors. Very large g-factors have been observed recently in semiconducting quantum wires and dots, where they represent the orbital contribution. [14–16] The difference between semiconducting wires or dots and our metallic particles is that the orbital contribution is quenched in the metallic particle. [17] The large g-factors described in this letter are of spin-origin, making the effect described herein different from that in semiconducting quantum dots and wires. This finding shows that a fundamental property of an electron, like the spin g-factor, can be strongly modified by the environment in an unexpected way.

EXPERIMENTAL METHODS AND DATA

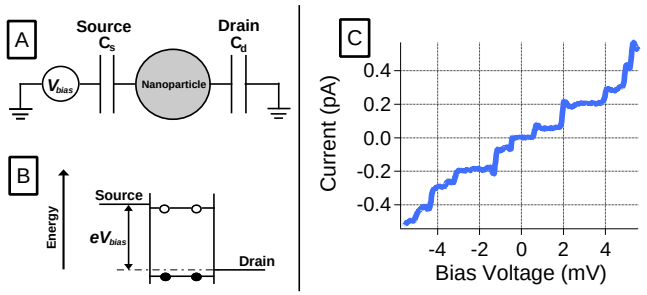

FIG. 1. Circuit diagram of tunneling through particle. B. Energy level diagram for tunneling process. C. IV curve displaying coulomb blockade and discrete single-electron tunneling steps.

Fig. 1-A sketches our arrangement for the studies of quantum levels and g-factors in a metallic particle. A single metallic particle is attached between two macroscopic leads, via high resistance tunnel junctions. Fig. 1-B displays the energy levels of the particle between the tunnel junctions. A voltage V_{bias} is applied on the source lead, changing the Fermi level in that lead by eV_{bias}. When the Fermi level in the source is equal to the energy difference between the final and the initial quantum state of the particle (after and before tunneling), an electron can tunnel from the Fermi level in the lead into the particle,

resulting in current flow. In that case the electrons flow through the particle one-by-one. Current versus voltage increases in discrete steps at the voltages where the Fermi level in the source equals the energy difference between the final and the initial quantum states of the particle, as our sample shows in Fig. 1-C. In most metallic particles, the energy difference between the final and the initial quantum state of the particle is equal to a discrete electron-in-a-box level in the particle. Thus, voltages at which the steps are observed in the I-V curve correspond to the discrete electron-in-a-box levels ϵ_μ. These levels are two-fold spin-degenerate, because of Kramers' theorem, and the degeneracy is lifted by the applied magnetic field. The g-factor is defined as in Ref. [12], by

$$g = \frac{\pm 2}{\mu_B}\frac{d\epsilon_\mu}{dB}. \quad (1)$$

The tunneling junction devices are fabricated using the same recipe quoted in Ref. 8. See Appendix A for more details. The devices are studied at T=60mK in a dilution refrigerator. The voltage bias is swept and the output current is measured using an Ithaco model 1211 current preamplifier. The detailed data sweeps involve a slow magnetic field ramp, along with a slightly faster sweep of the voltage bias. The differential conductance is calculated numerically. Fig. 2 displays our experimental data of the differential conductance vs. applied magnetic field and bias voltage for a Co sample. There are three main features of the data that are different from previous work on magnetic field dependence of tunneling spectra in a Co particle. First, the energy levels vs. magnetic field exhibit an abrupt change in slope around $B = 4$T. This kink was absent in prior work, which displayed energy levels that were monotonic with field in the range $B > 1$T. [8, 9, 18] Second, the g-factors of some levels in the figure are larger than 2. For example, the levels marked A and B in the figure correspond to g-factors of ≈ 7.3 at $B > 4$T. In comparison, prior work displayed only g-factors < 2 or ≈ 2 [8, 9, 18]. Finally, the fluctuations in the weights (i.e., the relative heights of the differential conductance peaks) of various levels is enhanced. Level A has a weight that is a factor of ≈ 4 smaller than level C, which displays a g-factor of ≈ 0.6. In Appendix C, additional data is provided, demonstrating the usual magnetic hysteresis loops of discrete levels in the low magnetic field range (< 1.5T). Because the energy level spacing of the Co particle is comparable to that of our previous work, we estimate the particle size to be ≈ 2nm . [8]

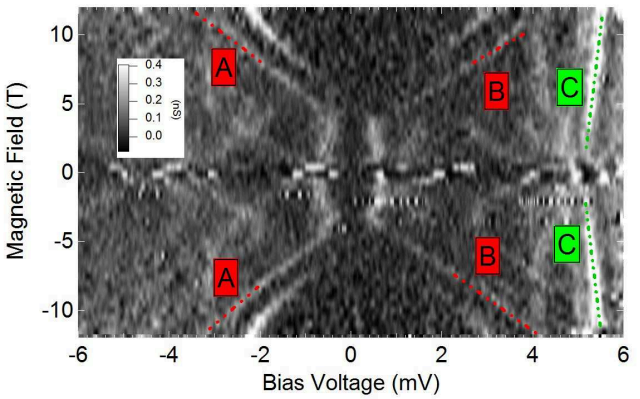

FIG. 2. Experimental data of differential conductance vs. magnetic field and bias voltage. The dotted lines follow the conductance peak behavior for two different spin transitions. The slope of the red dotted lines (A and B) yield a g-factor of ≈ 7.3, while the green dotted lines (C) correspond to a g-factor ≈ 0.6.

DATA MODEL: THE UNIVERSAL HAMILTONIAN

In this letter, we will present the analysis of electron tunneling through the particle, based on the Universal Hamiltonian (UH) model, and show how giant spin g-factors naturally arise in a ferromagnetic particle near spin degeneracies. [19] In the UH model, when the SO-interaction is zero, the electron-electron interaction commutes with the kinetic energy and the confinement potential, and the electronic energy in a metallic particle can be written as

$$E(N, S_0) = \sum_{\mu,\sigma=\uparrow,\downarrow} \epsilon_\mu n_{\mu,\sigma} - \frac{U}{2}S(S+1) - 2\mu_B B S_z, \quad (2)$$

where ϵ_μ is the energy of electron-in-a-box level μ, $n_{\mu,\sigma}$ is the occupation number for the level μ and spin direction σ, U is the exchange interaction, B is the magnetic field applied along z-axis, and S and S_z are the spin magnitude and its z-component, respectively, in units of $\hbar$. If the exchange interaction is small compared with the level spacing δ_μ at the Fermi level, then the ground state for this Hamiltonian will be the normal-metal Fermi sphere, with spin 0 or 1/2, depending on parity of the number of electrons on the particle (N). Giant spin g-factors can arise in the normal-metal state; however, their probability is very low. In the ferromagnetic state, the probability of giant g-factors increases dramatically; thus, we first analyze the ferromagnetic case.

Ferromagnetism occurs if the exchange interaction U is comparable to or larger than the level spacing $\delta_\mu = \epsilon_{\mu+1} - \epsilon_\mu$ at the Fermi level, and some minority electrons are promoted to higher level majority states. The maximum energies of the occupied levels will be labeled ϵ_m and ϵ_M (with corresponding level spacings δ_m and δ_M), for the minority and majority electrons, respectively. In the ground state, the exchange splitting between ϵ_m and ϵ_M is compensated by the gain in the exchange interaction energy: $\epsilon_M - \epsilon_m = U(S_0 + 1/2) + d(B)$. [20, 21] The

parameter $d(B)$ has magnetic field dependence $d(B) = d_0 - 2\mu_B B$, where d_0 is a mesoscopic parameter. Since the level spacings vary by the Wigner-Dyson statistics, the value of $\epsilon_M - \epsilon_m$ will have mesoscopic fluctuations comparable to $\delta_M + \delta_m$. Fig. 3-A depicts the N-electron ferromagnetic ground state with spin S_0. S_0 will be the ground state spin of the particle if $(U/2 - \delta_M) < d(B) < (\delta_m - U/2)$. At the applied magnetic field B_d, defined as $d(B_d) = U/2 - \delta_M$, the ground state is degenerate; that is, $E_N(S_0) = E_N(S_0 + 1)$. In a magnetic field slightly above B_d, the N-electron particle ground state spin will be $S_0 + 1$. The $S_0 + 1$ state is obtained from the diagram in Fig. 3-A, by annihilating the minority electron at energy ϵ_m and creating a majority electron at energy ϵ_{M+1}.

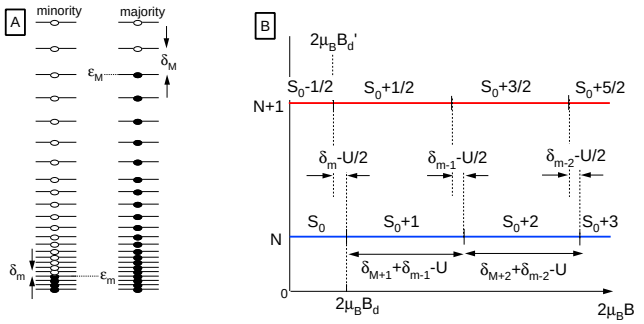

FIG. 3. A. Electron-in-a-box levels for minority and majority electrons. The black dots signify occupied levels. B. Stability Diagram for N- and (N+1)-electron particle. The spin value in each region denotes the ground state spin for the given magnetic field range. There is a degeneracy in ground state spin at $B = B_d$ and $B = B_d'$ for the N- and (N+1)-electron cases respectively.

As the magnetic field increases further, the transitions to higher spin states take place at the corresponding degeneracy fields. The stability regions for the ground state spins $S_0 + i$, $i = 0, 1, 2, ...$ are shown in Fig. 3-B.

In a Co particle, the average spacings and the exchange interaction are $\overline{\delta}_M = 4.58\text{eV}/S_0$, $\overline{\delta}_m = 1.18\text{eV}/S_0$, and $U = 1.77\text{eV}/S_0$, respectively. [21, 22] Note that the level spacings scale as $1/S_0$, which accounts for the vanishingly small level spacings as the electron number approaches typical bulk values. The magnetic field region (ΔB) for the stability of a particular spin is, on average, $2\mu_B \Delta B = \overline{\delta}_M + \overline{\delta}_m - U = 4\text{eV}/S_0$. For a typical Co particle in our experiment, $S_0 \approx 1000$, and the corresponding magnetic field range is quite large, $\Delta B \approx 35$T. Since our typical experimental field range of is ≈ 10T, we do not expect to observe spin degeneracy in a typical sample.

In an electron tunneling process, the number of electrons on the particle changes by one. In that case, if the particle spin before tunneling is S_0, then the final spin of the particle after the tunneling transition will be $S_0 \pm 1/2$. In Co, most tunneling transitions will be spin-lowering, as discussed previously. [8, 9, 18] Indeed, experimental studies of electron-in-a-box levels in Co particles done to date show that the levels from a given sample have roughly linear magnetic field dependence above about 1T, with similar g-factors < 2.

Fig. 3-B also displays the regions of stability for the ground state spins of $S_0 - 1/2 + i$, for the $(N+1)-$electron system. B_d' is the degenerate magnetic field value for the $(N+1)$-electron particle. Note that in most of the magnetic field range, the tunneling transition between the ground states reduces the spin by 1/2. However, in the narrow magnetic field range slightly below the degeneracy field B_d, the tunneling transition between the ground states will be spin-increasing, $S_0 \rightarrow S_0 + 1/2$. Such spin increasing tunnel transitions occur between $B = B_d'$ and $B = B_d$, where $g\mu_B(B_d - B_d') = \delta_m - U/2$. On average, $\langle B_d - B_d' \rangle / \Delta B = 0.07$. However, there is a prediction from the UH model that did not gain much attention until now, as far as we are aware. Because the level spacings fluctuate, there is a possibility that $(\delta_m - U/2)$ could be negative. In a Co particle, $\overline{\delta}_m = 1.33U/2$. Assuming the Wigner-Dyson distribution for δ_m, $\Pr[(\delta_m - U/2) < 0] = 36\%$ (See Appendix B). If $(\delta_m - U/2) < 0$, then in the magnetic field interval $[B_d, B_d']$, the ground state spins of the $N-$ and $(N+1)-$electron systems will be $S_0 + 1$ and $S_0 - 1/2$. In that case, the tunneling transitions between the ground states involve a spin-difference of 3/2, so the tunnel transition would display a g-factor of 6. Near any spin degeneracy, tunneling transitions between excited states can show large g-factors as well.

However, the tunnel Hamiltonian has zero-valued matrix elements between states of the particle with a spin difference other than $\pm 1/2$. That is, there is a spin selection rule $\Delta S = \pm 1/2$. But, if the SO-interaction in the particle is included, then the matrix elements $< S_0 - 1/2, S_0 - 1/2 | H_{SO} | S_0 + 1/2, S_0 + 1/2 >$ and $< S_0, S_0 | H_{SO} | S_0 + 1, S_0 + 1 >$ will be nonzero. For example, the calculation of the matrix element $< 3/2, 3/2 | H_{SO} | 1/2, 1/2 >$ is available in Ref. 12. [23]

The result is that the spin-eigenstates of the particle with N+1 electrons are 'spin' admixtures (hereafter labeled with a prime index) of pure states $|S_0 + 1/2, S_0 + 1/2 >$ and $|S_0 - 1/2, S_0 - 1/2 >$. Similarly, for the N electron system, states $|S_0, S_0 >$ and $|S_0 + 1, S_0 + 1 >$ mix. The closer the system is to spin-degeneracy, the stronger the admixing will become. The admixing produces two effects. First, the matrix elements of the tunnel Hamiltonian between $|S_0, S_0 >' \rightarrow |S_0 \pm 1/2, S_0 \pm 1/2 >'$ and $|S_0 + 1, S_0 + 1 >' \rightarrow |S_0 \pm 1/2, S_0 \pm 1/2 >'$, become nonzero. Now all tunneling transitions involving these four levels become active. If admixing is weak, then the weight of the transition $|S_0 + 1, S_0 + 1 >' \rightarrow |S_0 - 1/2, S_0 - 1/2 >'$ will be weak compared to the weight for transition $|S_0, S_0 >' \rightarrow |S_0 - 1/2, S_0 - 1/2 >'$. Similar variation in weights have been predicted before. [12] Second, the admixing will change the g-factors of the lev-

els. For example, we expect the g-factor for the transition $|S_0+1, S_0+1>' \rightarrow |S_0-1/2, S_0-1/2>'$ to be widely distributed around 6 and likely to remain much larger than 2, similar to the analysis in Ref. 12 and 13. However, there needs to be a more rigorous, full Random-Matrix-Theory description that includes orbital contributions to the g-factor in order to fully account for the value measured of 7.3.

Fig. 4-A,B sketches the energy versus magnetic field near the spin-degeneracy for the N- and $(N+1)$- electron systems. In the magnetic field range between B_d and B'_d indicated in the figure, the tunneling transition between the ground states involves a 'spin' change of $\Delta S' = 3/2$, and the g-factor should be about 6. Even if $B_d > B'_d$, the tunnel transition with $\Delta S' = 3/2$ will be close in energy. Thus, we expect to observe large g-factors for the transitions between the excited states, as long as the applied magnetic field is tuned near spin-degeneracy.

In a normal metal particle, the above analysis leads to a similar result. At the degeneracy field $B_{d,S-T}$ between singlet and triplet for the N-electron state (assuming N is even), the magnetic field is off degeneracy between doublet-quadruplet for the (N+1)-electron state by the amount given by $g\mu_B(B_{d,S-T} - B_{d,D-Q}) = \delta - U/2$. In order to observe a tunnel transition between ground state with spin-difference 3/2, $(\delta - U/2)$ needs to be less than zero. In contrast to the Co particle, U in a normal metal is small. For example, in a Au particle, $U/2 \approx 0.06\delta$, leading to the probability of 0.3% that the tunneling transition between ground states has $\Delta S' = 3/2$. [12] This is perhaps the reason no g-factors larger than two have been measured in a metallic particle, until now.

Moving back to Co particles, in order to measure large g-factors, we need to measure the particle near spin-degeneracy at the ground state. The experimental signature of the degeneracy would be a kink in the energy level versus magnetic field, according to Fig. 4-C,D. This is consistent with our data, where several levels display a kink near $B = 4$T. Our model also agrees with the predictions of Ref. 24, which discusses the signature kink in data near degeneracies, and is reminiscent of Ref. 25 and 26. Although the shape of the kink is not the exact same as that suggested by our simple model, the two have qualitatively good agreement. Additionally, we do not observe a second kink in the higher field range. However, due to the increasing intensity of the conductance peaks in the higher field range (which we attribute to stronger admixing between states), as well as a slight curvature of the lowest level near 12T, it is likely that a second kink lies beyond our magnetic field range.

CONCLUSION

In summary, we predicted the possibility of large spin-g-factors of a ferromagnetic particle tuned close to spin-degeneracy. The existence of these giant effective g-factors is due to the many-body interactions (i.e., strong exchange energy) in a ferromagnetic particle. When tuned within a certain range, the magnetic field induces a degenerate total spin value on the particle. Due to fluctuations in the electron-in-a-box level spacings, there is a significant probability that this magnetic field range, along with spin-orbit interactions, can allow transitions that change the 'spin' of the particle by 3/2 upon the tunneling event of a single electron. However, this will only occur if the magnetic field is tuned sufficiently close to one of these degenerate field values. We prepared many samples of cobalt particles, and found the experimental signature of a degenerate magnetic field value (the kink in the conductance data plot). Within this data set, we found very large g-factors (g≈ 7.3), in relatively close agreement with our prediction. These giant spin-g-factors display the intricate interplay between the many-body energy states and the traditional electron-in-a-box quantum states.

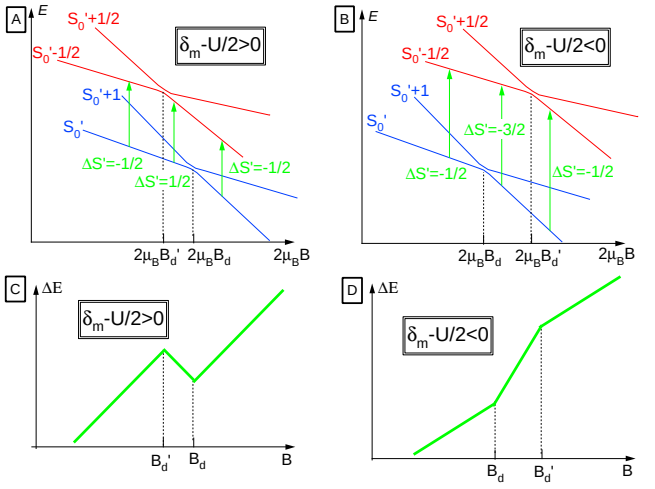

FIG. 4. Possible spin transitions upon the tunneling event of a single electron onto the particle. The length of the arrows represent the energy change of the particle upon such a transition. A. Case where $B'_d < B_d$, $(\delta_m > U/2)$. B. Case where $B'_d > B_d$, $(\delta_m < U/2)$. C,D. Kink in energy curve as a function of B for the two cases considered in A,B.

ACKNOWLEDGMENTS

We would like to thank Y. Ding from the School of Materials Science and Engineering at Georgia Institute of Technology for his help in taking the TEM image of the Co particles. This work has been supported by the Department of Energy (DE-FG02-06ER46281).

APPENDICES

Appendix A: Sample Fabrication

The structures of our samples are defined using electron-beam lithography on a poly(methyl methacrylate)(PMMA) substrate, as is illustrated in Fig. 5.

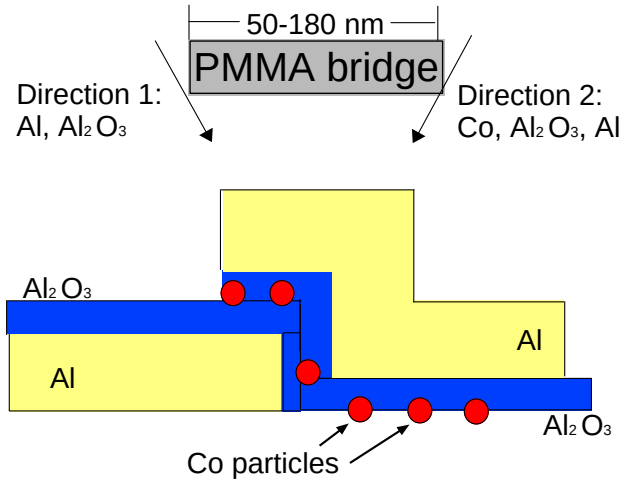

FIG. 5. Sample fabrication process. The cobalt particles are shown in red between the two tunneling barriers (blue) and the conducting Al electrodes (yellow)

After exposure to the electron-beam, the sample is placed in developer solution and a bridge of PMMA is established for use in shadow evaporation. Next, the sample is placed in a vacuum chamber and the tunnel junctions are created through shadow evaporation around the PMMA bridge. Aluminum is evaporated to form the electrode, followed by a a layer of Al_2O_3 to form the first tunneling barrier. Next, the sample is rotated and a layer of Cobalt on the order of 0.6 nm is added, which nucleates due to surface tension and forms the nanoparticles to be studied. A second layer of Al_2O_3 is then added to form the other tunnel junction, and then a final layer of Al is evaporated to form the other electrode. The electrodes are ≈ 14 nm thick, and the Al_2O_3 tunnel junctions are ≈ 1.7 nm thick. After the evaporation process, the excess metals are lifted off in acetone, leaving a series of patterned devices on our substrate. The nanoparticles are pictured in Fig. 6 in a Transmission Electron Microscope (TEM) micrograph.

Appendix B: Wigner-Dyson Statistics

The energy level statistics of electrons occupying chaotic wavefunctions on the quantum dot can be modeled using Random Matrix Theory (RMT) and Wigner-Dyson statistics. For our model, we use the Gaussian

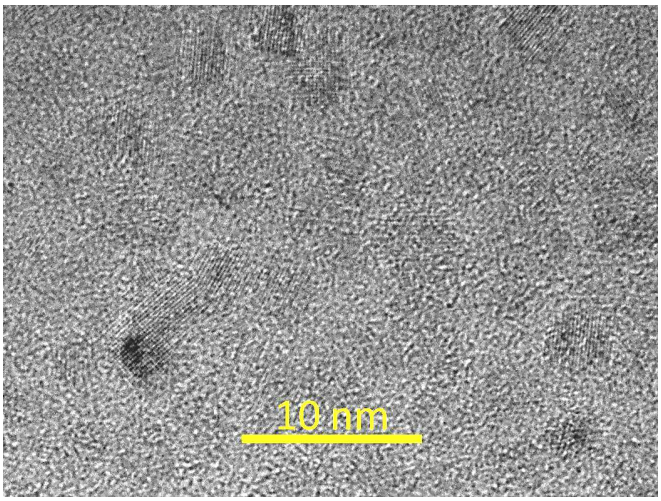

FIG. 6. TEM image of Co nanoparticles (dark) on amorphous Al_2O_3 background (light)

Orthogonal Ensemble (GOE) because we are in the low magnetic field regime and therefore can treat the system as effectively time-reversal invariant. Modeling the system with the Gaussian Unitary Ensemble (GUE), which is the ensemble that should be used for systems without time-reversal symmetry, was also performed, but the results for GOE and GUE have a difference of only a few percent. The GOE has normalized energy level $\left(x \equiv \frac{\delta_m}{\langle \delta_m \rangle}, \text{ where } \langle \delta_m \rangle \equiv \overline{\delta}_m\right)$ fluctuations that follow the distribution function $F(x)$:

$$F(x) = \frac{\pi}{2} x e^{-\frac{\pi}{4}x^2} \tag{3}$$

So to find the probability, Pr, that $(\delta - U/2)$ is negative, we note:

$$\Pr\left((\delta_m - \frac{U}{2}) < 0\right) =$$

$$\Pr\left((\frac{\delta_m}{\langle \delta_m \rangle} - \frac{U/2}{\langle \delta_m \rangle}) < 0\right) =$$

$$\Pr\left((x - \frac{U/2}{1.33U/2}) < 0\right) =$$

$$\Pr\left((x - 0.75) < 0\right) =$$

$$\Pr\left(x < 0.75\right) = \int_0^{0.75} \mathrm{d}x \frac{\pi}{2} x e^{-\frac{\pi}{4}x^2} \approx 36\%$$

A similar calculation using the GUE instead yields a probability of $\approx 30\%$. Either way, there is non-negligible probability that the quantity $(\delta - U/2)$ will be negative.

Appendix C: Low Magnetic Field Data (< 1.5T)

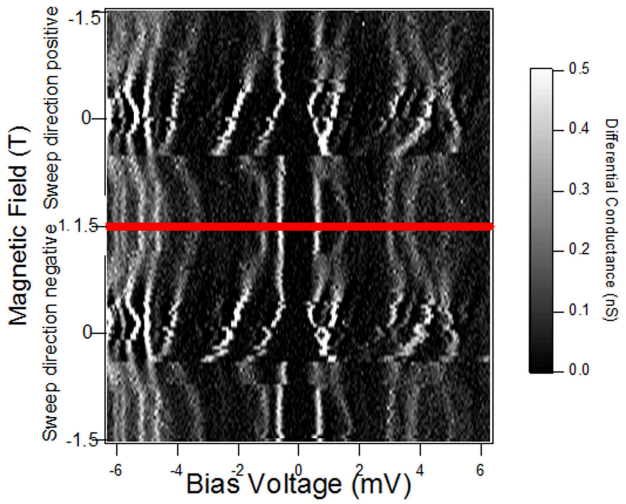

FIG. 7. Low Magnetic Field Data < 1.5 T

The data shown in Fig. 7 displays the low magnetic field regime of the differential conductance vs. voltage. Over time, the field was swept from $-1.5 \rightarrow +1.5$T, and then from $+1.5 \rightarrow -1.5$T. This is shown in the graph by reading it from top to bottom. The discontinuities in the conductance data for the same bias voltage values indicate that a magnetic switch has occurred. Note the hysteresis in the switching field values— when the field is swept from negative values to positive ones, the switch occurs in the positive magnetic field range. Conversely, when the field is swept from positive to negative values(the lower half of the graph) the switch occurs for negative field values. These characteristics indicate that we are indeed measuring the tunneling through a single ferromagnetic particle, and agree qualitatively with previous work on Co particles[8].

* Author to whom correspondence should be addressed. E-Mail: pgartland3@gatech.edu

[1] D. Davidović and M. Tinkham, Phys. Rev. Lett. **83**, 1644 (1999).

[2] D. G. Salinas, S. Gueron, D. C. Ralph, C. T. Black, and M. Tinkham, Phys. Rev. B **60**, 6137 (1999).

[3] R. C. Ashoori, Nature **379**, 413 (1996).

[4] M. A. Kastner, Phys. Today **46**, 24 (1993).

[5] D. C. Ralph, C. T. Black, and M. Tinkham, Phys. Rev. Lett. **74**, 3241 (1995).

[6] D. C. Ralph, C. T. Black, and M. Tinkham, Phys. Rev. Lett. **78**, 4087 (1997).

[7] C. T. Black, D. C. Ralph, and M. Tinkham, Phys. Rev. Lett. **76**, 688 (1996).

[8] W. Jiang, F. T. Birk, and D. Davidovic, Sci. Rep. **3**, 1200 (2013).

[9] M. M. Deshmukh, S. Kleff, S. Gueron, E. Bonet, A. N. Pasupathy, J. von Delft, and D. C. Ralph, Phys. Rev. Lett **87**, 226801 (2001).

[10] K. A. Matveev, L. I. Glazman, and A. I. Larkin, Phys. Rev. Lett. **85**, 2789 (2000).

[11] S. Adam, M. L. Polianski, X. Waintal, and P. W. Brouwer, Phys. Rev. B **66**, 195412 (2002).

[12] D. A. Gorokhov and P. W. Brouwer, Phys. Rev. B **69**, 155417 (2004).

[13] D. A. Gorokhov and P. W. Brouwer, Phys. Rev. Lett. **91**, 186602 (2003).

[14] H. A. Nilsson, P. Caroff, C. Thelander, M. Larsson, J. B. Wagner, L.-E. Wernersson, L. Samuelson, and H. Q. Xu, Nano Letters **9**, 3151 (2009), pMID: 19736971, http://pubs.acs.org/doi/pdf/10.1021/nl901333a.

[15] S. Nadj-Perge, V. S. Pribiag, J. W. G. van den Berg, K. Zuo, S. R. Plissard, E. P. A. M. Bakkers, S. M. Frolov, and L. P. Kouwenhoven, Phys. Rev. Lett. **108**, 166801 (2012).

[16] M. D. Schroer, K. D. Petersson, M. Jung, and J. R. Petta, Phys. Rev. Lett. **107**, 176811 (2011).

[17] The assumption that the orbital angular momentum is quenched in a metal particle is based upon the work by Matveev and Adam,[10, 11] wherein they calculate the orbital contribution to the g-factor for a range of SO strengths, as well as for diffusive and ballistic transport. In the case of zero SO interaction, there is no contribution to the orbital g-factor because the magnetic field required to add a magnetic flux quantum over the area of our sample is $\approx$ 1000T. When SO$\neq$ 0, the orbital contribution for a ballistic nanoparticle is on the order of $\left(\frac{m}{m^*}\right)^2$, where m and m^* are the electron mass and effective mass, respectively. Because the effective mass is enhanced for the narrow d-band of Cobalt, this orbital contribution term will not be $\gg 1$. For the diffusive particle case, the orbital contribution will be even smaller.

[18] S. Gueron, M. M. Deshmukh, E. B. Myers, and D. C. Ralph, Phys. Rev. Lett. **83**, 4148 (1999).

[19] I. Aleiner, P. Brouwer, and L. Glazman, Physics Reports **358**, 309 (2002).

[20] A. MacDonald and C. Canali, Solid State Communications **119**, 253 (2001).

[21] C. M. Canali and A. H. MacDonald, Phys. Rev. Lett. **85**, 5623 (2000).

[22] D. Papaconstantopoulos, *Handbook of the band structure of elemental solids* (Plenum Press New York, 1986).

[23] That calculation can be extended in a straightforward way to our states with large S_0, but would be beyond the present scope. In a ferromagnetic particle with large S_0, many of the matrix elements of H_{SO} calculated in Ref. 12 become negligibly small in the thermodynamic limit. For example, while $< S_0+1, S_0+1|H_{SO}|S_0, S_0 >$ and $< 3/2, 3/2|H_{SO}|1/2, 1/2 >$ are comparable, $< S_0+1, S_0|H_{SO}|S_0, S_0 >$ is smaller by factor of $\sim 1/\sqrt{2S_0}$ compared to $< 3/2, 1/2|H_{SO}|1/2, 1/2 >$. The SO-interaction becomes a tri-diagonal matrix connecting only spin ground states, while the matrix elements connecting different magnetically excited levels can be neglected.

[24] H. U. Baranger, D. Ullmo, and L. I. Glazman, Phys. Rev. B **61**, R2425 (2000).

[25] A. Kogan, G. Granger, M. A. Kastner, D. Goldhaber-Gordon, and H. Shtrikman, Phys. Rev. B **67**, 113309 (2003).

[26] S. Tarucha, D. G. Austing, Y. Tokura, W. G. van der Wiel, and L. P. Kouwenhoven, Phys. Rev. Lett. **84**, 2485 (2000).